

SCREENING TESTS FOR ENHANCED SHIELDING AGAINST HYPERVELOCITY PARTICLE IMPACTS FOR FUTURE UNMANNED SPACECRAFT

Robin Putzar⁽¹⁾, Jan Hupfer⁽¹⁾, Gwenaëlle Aridon⁽²⁾, Bernard Gergonne⁽²⁾,
Matthieu David⁽³⁾, Paul Bourke⁽⁴⁾, Claude Cougnet⁽²⁾

⁽¹⁾ Fraunhofer Institute for High-Speed Dynamics, Ernst-Mach-Institut, EMI,
Eckerstr. 4, 79104 Freiburg, GERMANY, Email: robin.putzar@emi.fraunhofer.de

⁽²⁾ Astrium Satellites, 31 Avenue des Cosmonautes, 31404 Toulouse, FRANCE

⁽³⁾ Astrium Satellites, Claude-Dornier-Straße, 88090 Immenstaad, GERMANY

⁽⁴⁾ TenCate Advanced Armour, Murdock Rd, Dorcan, Swindon, SN3 5HY Wiltshire, UNITED KINGDOM

ABSTRACT

Protection of components of unmanned spacecraft against particle impacts is typically provided by the spacecraft's structure together with the intrinsic protection capabilities of the components themselves. Thus to increase the survivability of future spacecraft, one option is to enhance the protection already provided using enhanced materials and additional shielding.

As part of the EU funded FP7 research project ReVuS ("Reducing the Vulnerability of Space systems"), the configurations of equipment typically found on board unmanned spacecraft were identified. For each of those configurations, potential solutions have been identified which enhance the robustness against particle impacts. The solutions are broken down into a number of shielding components that include e.g. additional protective layers made from aluminum, Kevlar, Nextel, stainless steel mesh and ceramics. To evaluate the characteristics and performances of these shielding components, a number of screening hypervelocity impact tests were performed. During these tests, representative configurations have been subjected to impacts of aluminum spheres of 3 mm and 5 mm diameter at a nominal impact velocity of 7 km/s.

This paper describes the targets and presents and compares the results.

1 INTRODUCTION

Micrometeoroid and space debris (MMSD) particles pose a significant threat to unmanned spacecraft. Particles with a size of one millimeter perforate typical unmanned spacecraft structure walls and subsequently can damage or destroy components inside [1-4]. Depending on the components' relevance, a single impact can lead to termination of a mission. Impacts of larger fragments lead to disintegration of spacecraft parts [5] or the whole spacecraft [6], generating new debris.

Protection of components of unmanned spacecraft against particle impacts is typically provided by the spacecraft's structure together with the intrinsic protection capabilities of the components themselves. Thus to increase the survivability of future spacecraft, one option is to enhance the protection already provided using enhanced materials and additional shielding.

2 THE REVUS PROJECT

The aim of the EU FP7 funded ReVuS project ("Reducing the Vulnerability of Space systems") is to identify ways to improve the resilience of space systems to a collision with small debris, thus to reduce the risk of partly or fully the mission. The ReVuS project is presented in [7].

The ReVuS consortium consists of Astrium SAS in Toulouse, Fraunhofer Ernst-Mach-Institut in Freiburg, Technische Universität Braunschweig, University of Southampton, University of Leicester, Astrium GmbH in Friedrichshafen, PHS Space Ltd. in Pitlochry, TenCate Advanced Composites in Nijverdal, Hiscox Global Risks Europe in Paris and Astri Polska in Warsaw. The ReVuS project website is <http://www.revus-project.eu/>.

The project logic follows a three step approach: (1) evaluation of the threat and of the risks on a satellite and of potential consequences on the mission, (2) identification and analysis of potential solution at system and spacecraft levels, including protective shielding, and (3) evaluation of the performances of the selected solutions with respect to the threat (resilience) and proposal of design rules and standards.

Step (2) is divided into three large work packages: system level solutions, spacecraft configuration solutions and shielding technology solutions.

Within the shielding technology solution work package, two test campaigns are foreseen. The first campaign is a preparatory campaign in which materials are tested and

compared for their efficiency. In the second campaign, entire shielding configurations are tested and compared. This paper is about major results from the first test campaign.

3 IMPACT TEST PREPARATION

3.1 TEST RATIONALE

The aim of the first test campaign is to evaluate promising shielding components identified during the study. Each shielding component is placed within a set-up that is representative for its occurrence within a spacecraft: multi-layer insulation (MLI) and sandwich panel samples are placed at the outermost location and impacted directly, whereas intermediate layer samples are placed with some spacing behind a bumper. The targets are impacted with similar impact conditions above their ballistic limit. Behind each target, witness plates are placed. Witness plate 1 (WP1) is considered somewhat representative for module walls.

To be able to test a great variety of different materials, an approach similar to the one presented in [8] (also used in [9]) is used. In [8], a damage number was introduced to compare bumpers. Bumpers composed of different materials but having the same areal density were placed 50.8 mm (2 inches) in front of a 1.27 mm (0.05 inches) Al 2024-T3 module wall. 100 mm behind the module wall, a 0.4 mm thick Al 3003-0 witness plate was installed. This damage number incorporated the total hole area of the module wall and damage to the witness plate.

In the approach of this paper, the penetration capability of the most damaging fragment impacting WP1 (representing the module wall) is estimated. The approach is detailed in section 5 below.

3.2 Target set-up

The target set-up depends on the type of shielding component to be investigated. In each target, the corresponding component is placed in a set-up that is representative for its occurrence within a spacecraft. Each target set-up contains the component to be investigated plus a number of witness plates. For “MLI” and “sandwich panel” shielding components, the component is placed like a bumper, i. e. impacted first. For “intermediate layers or reinforced box wall” components, an aluminum (Al) bumper plate is added to ensure that the component is impacted by a fragment cloud. Aluminum has been proven to produce very homogeneous fragment clouds, generating very reproducible conditions for all intermediate layer tests.

Figs. 1 and 2 show the corresponding target set-ups for testing of the shielding components.

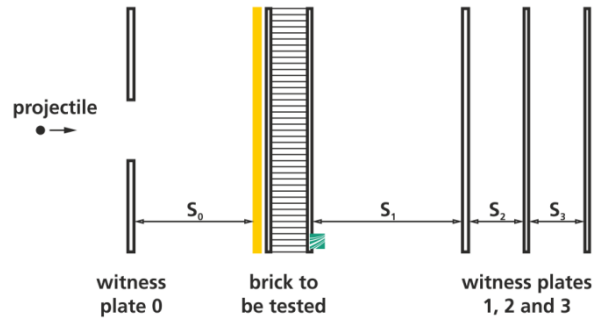


Figure 1. Target set-up for shielding components “MLI” and “sandwich panel”.

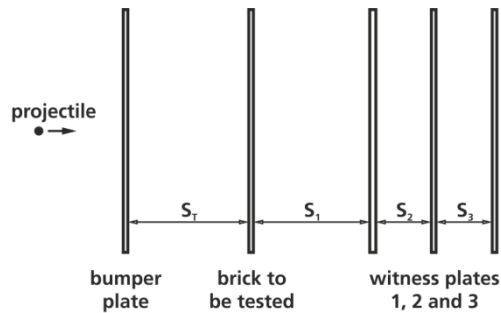


Figure 2. Target set-up for shielding component “intermediate layer or reinforced box wall”.

The first witness plate (WP0) is placed in up-range direction to monitor material ejected outside the spacecraft during impact events. This is a 2.0 mm thick Al 2024 clad T351 sheet.

The first witness plate behind the component (WP1) is a 2.0 mm thick Al 2024 clad T351 sheet. This sheet is representative for a module wall. Thus, the damage of the first witness plate gives an indication of the damage to a module behind the respective shielding component.

WP0 and WP1 are painted black to help damage evaluation.

All further witness plates (WP2 and WP3) are 0.5 mm thick Al 2024 clad T3 sheets. These witness plates are used to monitor residual damage capabilities of the fragment cloud or detached spallation behind the first witness plate.

Spacing between WP1 and WP2 and between WP2 and WP3 is 20 mm.

3.3 Target description

Four investigated target types are presented in this paper: “multi-layer insulation” (MLI), “aluminum sandwich panels”, “CFRP sandwich panels” and “intermediate layer or reinforced box wall”.

3.3.1 MLI

Baseline multi-layer insulation (MLI) (target 1.1) consists of one 50.8 μm (2 mil) Kapton layer with vapor deposited aluminum (VDA) outside, eight 6.35 μm (0.25 mil) Mylar/VDA layers and one 25.4 μm (1 mil) Mylar/VDA layer inside. The Kapton/Mylar layers are separated by nine Dacron spacer layers.

The other MLI targets consist of the same baseline MLI with additional layers:

- Target 1.2: baseline MLI with two layers of Nextel placed behind
- Target 1.3: baseline MLI with two layers of heavy stainless steel mesh placed behind
- Target 1.3-2: baseline MLI with two layers of light stainless steel mesh placed behind
- Target 1.4: baseline MLI with one layer of heavy stainless steel mesh and one layer of Nextel placed behind
- Target 1.4-2: baseline MLI with one layer of light stainless steel mesh and one layer of Nextel placed behind
- Target 1.5: baseline MLI with one layer of Aramid plus second baseline MLI placed at 20 mm stand-off distance with one layer of Nextel
- Target 1.6: baseline MLI with one layer of Aramid plus second baseline MLI placed at 20 mm stand-off distance with one layer of heavy steel mesh.

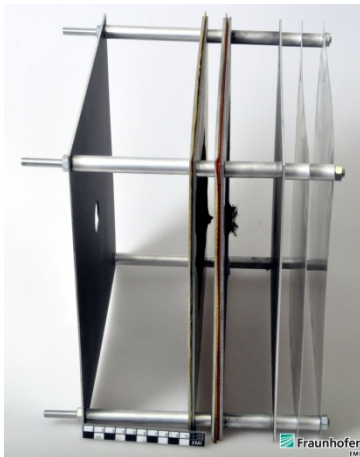


Figure 3. Example MLI target (no. 1.6, experiment 5397) after impact testing.

3.3.2 Aluminum sandwich panel

Baseline aluminium (Al) sandwich panel (SP) (target 2.1) consists of two 0.5 mm skins from Al 2024 T3 and 40 mm Al 5056-3/16-0.001 honeycomb core in between. The other Al SP targets deviate from this as given in the following list:

- Target 2.2: baseline Al SP with two additional 0.5 mm Al 2025 T3 sheets, one glued to the outside and one glued to the inside
- Target 2.3: baseline Al SP with one additional 0.5 mm Al 2025 T3 sheet placed in the center of the Al honeycomb core such that the honeycomb core consists of two individual layers of 20 mm thickness each
- Target 2.4: baseline Al SP with the two face sheets replaced by two sheets consisting of a 0.25 mm layer of Al 2024 T3, a 0.5 mm layer of Al_2O_3 and a 0.25 mm layer of Al 2024 T3
- Target 2.5: baseline Al SP with two layers of heavy stainless steel mesh placed behind
- Target 2.6: baseline Al SP with 40 mm Al foam inside instead of a honeycomb core.



Figure 4. Example aluminum sandwich panel target (no. 2.3, experiment 5387) before impact testing.

3.3.3 CFRP sandwich panel

Baseline carbon-fiber reinforced plastic (CFRP) sandwich panel (Target 3.1) consists of two 4-ply CFRP skins with 40 mm Al 5056-3/16-0.001 honeycomb core in between. The CFRP skins consist of 4 plies of 200 g/m^2 plain weave, 3K Carbon fibers (orientation [0-90], [0-90], [0-90], [0-90]) with a RP400 epoxy resin.

Target 3.2 differs from Target 3.1 in that the CFRP skins have been reinforced with tungsten carbide (WC) particles.

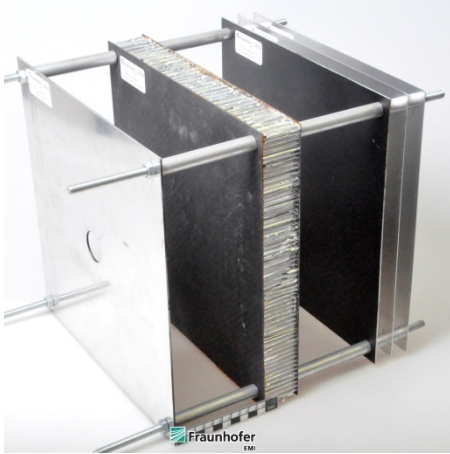


Figure 5. Example CFRP sandwich panel target (no. 3.2, experiment 5404) before impact testing.

3.3.4 Intermediate layer or reinforced box wall

The following targets have been tested as intermediate layer or reinforced box wall:

- Target 5.1: An Al 2024 T3 sheet with 0.5 mm thickness
- Target 5.2: three layers of Aramid
- Target 5.3: two layers of Nextel and one layer of Aramid
- Target 5.5: on layer of Aramid embedded within thermoplastic.

Each layer is preceded by a 1.0 mm Al 2024 T3 bumper plate. The mass of this bumper plate is included in the areal density of the target.



Figure 6. Example intermediate layer or reinforced box wall target (no. 5.2, experiment 5392) before impact testing.

3.3.5 Overview

Tab. 1 shows an overview of all impacted targets with their respective parameters. In case S_0 is not given in the table, no witness plate 0 was used in the respective target.

Table 1: Target overview. S_0 = spacing to witness plate 0, S_T = spacing inside target, S_1 = spacing from target to witness plate 1, AD = areal density.

No.	Short description	S_0 [mm]	S_T [mm]	S_1 [mm]	AD [kg/m ²]
1.1	MLI	100	–	50	0.27
1.2	MLI+2×Nextel	100	–	50	0.80
1.3	MLI+2×heavy mesh	100	–	50	3.77
1.3-2	MLI+2×light mesh	100	–	50	0.85
1.4	MLI+heavy mesh+ Nextel	100	–	50	2.29
1.4-2	MLI+light mesh+Nextel	100	–	50	0.83
1.5	MLI+Aramid+20mm +MLI+Nextel	100	20	50	1.25
1.6	MLI+Aramid+20mm +MLI+heavy mesh	100	20	50	2.73
2.1	Al SP	–	–	250	4.92
2.2	Al SP+2×0.5 mm skins	–	–	250	7.88
2.3	Al SP+0.5 mm inner Al layer	100	–	250	6.48
2.4	Al SP with Al ₂ O ₃ skins	–	–	250	9.18
2.5	Al SP+2× heavy mesh	100	–	250	8.38
2.6	Al SP with foam	–	–	250	7.85
3.1	CFRP SP	100	–	100	4.71
3.2	CFRP SP with WC	100	–	100	8.84
5.1	Al layer	100	50	50	4.20
5.2	3× Aramid	100	50	50	4.15
5.3	2× Nextel, 1× Aramid	–	50	50	3790
5.5	1× Aramid within thermoplastic	–	50	50	4580

3.4 Test parameters

The impact parameters were chosen so that the component is perforated. Impacting projectiles were spheres of 99.9 % pure aluminum. All impact tests were performed at 7 km/s. All impacts were performed at 0° incidence, measured from surface normal. This is the most damaging case.

During the ReVuS study, particle sizes that the shield should withstand were defined for three different types of equipment that the corresponding shield should withstand: 1 mm at 15 km/s for external units and 3 mm at 15 km/s for internal units. The particle sizes are scaled to 7 km/s using a kinetic energy approach as is commonly used with ballistic limit equations: In this approach, the diameter scales with the power of two thirds of the velocity ratio:

$$E_{\text{kin}} \sim m \cdot v^2 \sim d^3 \cdot v^2 \Leftrightarrow d \sim v^{-\frac{2}{3}} \quad (1)$$

The external equipment type corresponds to the shielding component “MLI”. For this component, the kinetic energy approach leads to a projectile size of 1.7 mm at 7 km/s. This particle size was considered too small to cause enough damage on the witness plate for a useful comparison of the protective capabilities of different targets. Thus, a projectile size of 3.0 mm at 7 km/s was chosen.

The internal equipment type corresponds to the remaining shielding components investigated, i. e. “sandwich panel” and “intermediate layer or reinforced

box wall”. For this equipment, the kinetic energy approach leads to a 5 mm projectile size. This size was considered to cause enough damage to allow for a useful comparison of the target witness plates.

4 TEST RESULTS

Test results are shown in Tab. 2. For the analysis, the maximum crater depth in WP1 as well as the amount of perforated witness plates is important.

Fig. 7 shows some targets after impact testing.

Table 2: Test parameters and results. Exp. = experiment number, d_p = projectile diameter, m_p = projectile mass, v_p = impact velocity, AD = areal density.

Exp.	Target	d_p [mm]	m_p [mg]	v_p [km/s]	Short damage description	Penetrated AD [kg/m ²]
5379	1.1	3.0	37.1	6.8	WP1: hole \varnothing 9.7 mm; WP2: perforation; WP3: craters	13.30
5380	1.2	3.0	36.8	6.7	WP1: hole \varnothing 10.4 mm; WP2: perforation; WP3: craters	13.83
5381	1.3	3.0	37.1	7.0	WP1: max. crater depth 0.6 mm	6.15
5411	1.3-2	3.0	37.2	7.4	WP1: hole 9.4 mm x 11.7 mm; WP2: perforation; WP3: perforation	13.88
5382	1.4	3.0	37.0	7.0	WP1: max. crater depth 1.4 mm	7.85
5424	1.4-2	3.0	37.1	7.0	WP1: hole 10.2 mm x 11.3 mm; WP2: perforation; WP3: craters	13.86
5383	1.5	3.0	37.2	7.2	WP1: hole \varnothing 1.6 mm; WP2: deposit	9.94
5397	1.6	3.0	37.3	7.1	WP1: max. crater depth 0.75 mm	5.71
5375	2.1	5.0	177.3	7.0	WP1: hole \varnothing 1.4 mm; WP2: deposit	13.61
5378	2.2	5.0	177.3	7.0	WP1: hole \varnothing 3.3 mm; WP2: deposit	16.57
5387	2.3	5.0	177.7	7.0	WP1: max. crater depth 0.7 mm	9.26
5377	2.4	5.0	177.3	7.0	WP1: max. crater depth 0.74 mm	12.12
5398	2.5	5.0	177.8	7.1	WP1: max. crater depth 1.1 mm	12.75
5376	2.6	5.0	177.1	7.0	WP1: max. crater depth 0.13 mm	8.36
5403	3.1	5.0	177.4	7.1	WP1: hole \varnothing 7.0 mm; WP2: perforation; WP3: perforation	17.74
5404	3.2	5.0	178.2	7.1	WP1: max. crater depth 0.1 mm	9.24
5391	5.1	5.0	177.4	6.9	WP1: max. crater depth 0.6 mm	6.58
5392	5.2	5.0	177.4	6.9	WP1: deposit / max. crater depth 0.05 mm	4.35
5394	5.3	5.0	177.9	7.2	WP1: deposit / max. crater depth 0.05 mm	3.99
5395	5.5	5.0	177.1	7.1	WP1: max. crater depth 0.15 mm	5.18



Figure 7. Example targets after impact testing. From left to right: aluminum sandwich panel (Target 2.3, experiment 5387), CFRP sandwich panel (Target 3.2, experiment 5404), intermediate layer or reinforced box wall (Target 5.2, experiment 5392).

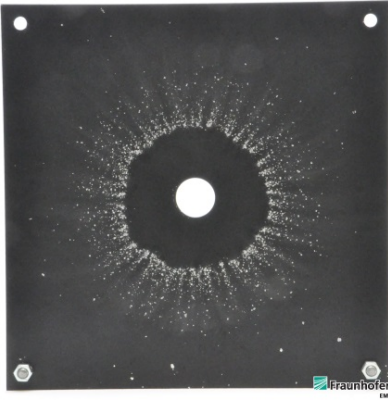


Figure 8. WP0 (ejecta catcher) of Sample 5.2 (Experiment 5392).

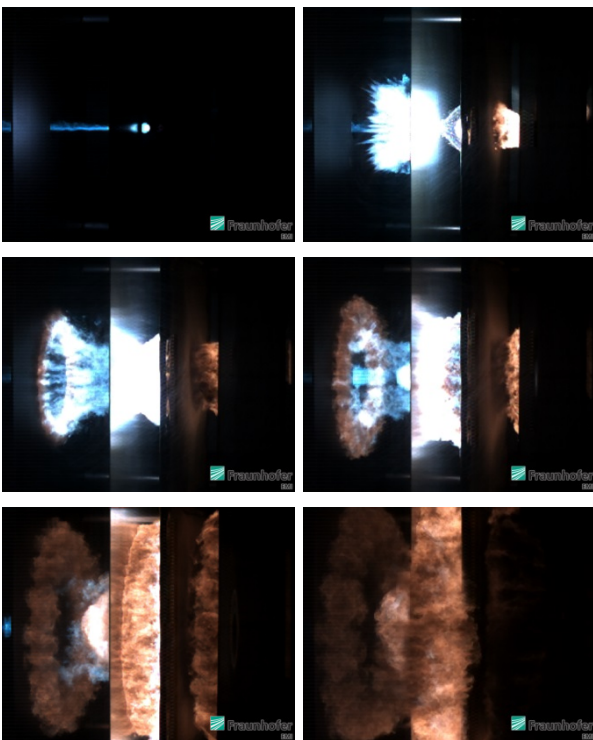


Figure 9. High-speed video images from Experiment 5392 (Sample 5.2). Image times with respect to impact are 1 μ s, 19 μ s, 38 μ s, 56 μ s, 112 μ s and 223 μ s.

5 TEST ANALYSIS

As all targets are different, comparison of their performance is nontrivial. In this paper, the penetration capability of the most damaging fragment impacting WP1 (the witness plate simulating the module wall) is estimated. This penetration capability is a measure for the quality of the investigated sample. This parameter describes both the sample's ability to disperse the fragment cloud over a larger area, and (especially for

intermediate layer samples) to decrease a fragment cloud's energy.

For targets where WP1 is not perforated, the penetration capability is the crater depth in this witness plate. For targets where WP1 is perforated but WP2 is not, the penetration capability is assumed to be that of a sphere being capable to perforate WP1 only, calculated with the Cour-Palais damage equation as presented in [10]. For targets where WP1 and WP2 are perforated but WP3 is not, the penetration capability is assumed to be that of a sphere being capable to perforate a Whipple shield made up of WP1 and WP2. According to [10], the diameter of such a sphere is approx. 125 % that of a sphere being able to perforate a single plate with a thickness equal to the sum of the two witness plate thicknesses. For targets where all three witness plates are perforated, the penetration capability is assumed to be 1.25² times that of a sphere being able to perforate a plate having a thickness equal to the sum of all three witness plates.

The penetration capability is given in terms of the penetrated areal density of the shield. This number includes the (nominal) areal density of all layers that would have been necessary to stop the impacting particle. The module wall (represented by WP1 in the experiments) is calculated from the perforation capability of the most damaging fragment as identified by the procedure outlined above, using the Cour-Palais damage equation. For a target where WP1 is perforated but WP2 not, it is equal to the areal density of all layers up to, but excluding WP1, plus 125 % of the sum of the areal density of WP1 and WP2. For a target where WP1 is not perforated, it is a plate having a thickness 1.5 times the depth of the deepest crater found in the witness plate.

Figs. 10 to 13 show the so-obtained penetrated areal density plotted versus the areal density of the sample. A higher penetrated areal density indicates worse performance of the investigated sample. Thus, the best samples are found at the bottom of the graph. Filled symbols indicate that WP1 was perforated for the respective sample; while open symbols indicate that the fragments were stopped by WP1. The identity is included in all figures as a solid line. Thus, the penetrated witness plate areal density, which is also an interesting parameter to consider, can be easily estimated from the figures by the distance of the datapoints to this line.

It should be noted that comparison of penetrated areal densities between the four sample types ("MLI", "Al sandwich panel", "CFRP sandwich panel" and "intermediate layers or reinforced box wall") is limited due to different impact conditions for each sample type (particle diameter, stand-off to WP1). Within each

sample group, the impact conditions have been kept nominally constant.

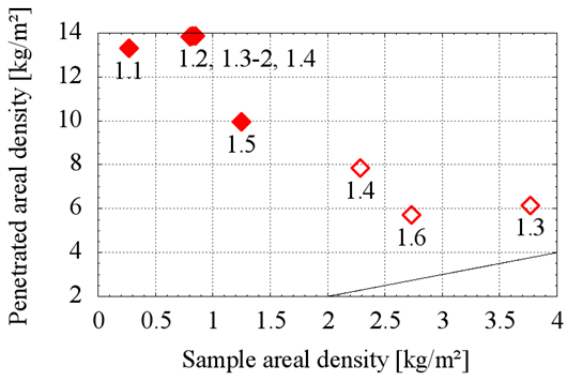


Figure 10. Penetrated areal density plotted vs. sample areal density for the “MLI” targets. Filled symbols indicate WPI perforation. Solid line is identity.

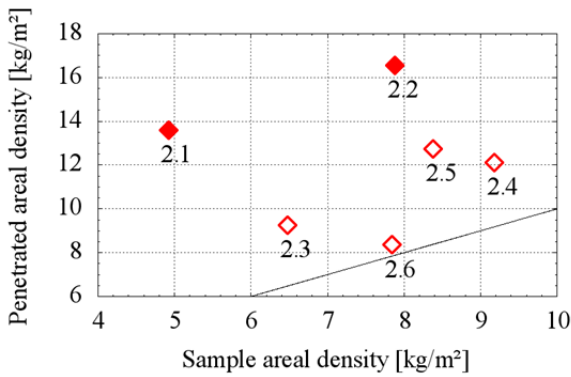


Figure 11. Penetrated areal density plotted vs. sample areal density for the “Al sandwich panel” targets. Filled symbols indicate WPI perforation. Solid line is identity.

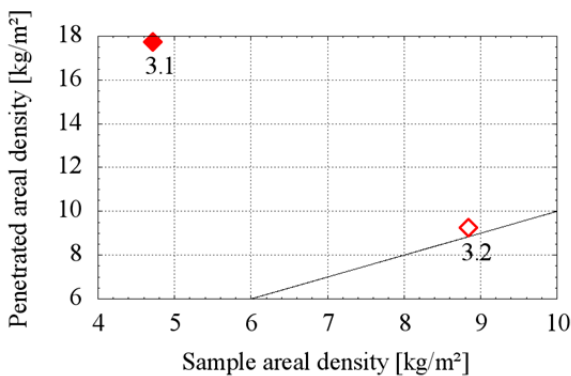


Figure 12. Penetrated areal density plotted vs. sample areal density for the “CFRP sandwich panel” targets. Filled symbols indicate WPI perforation. Solid line is identity.

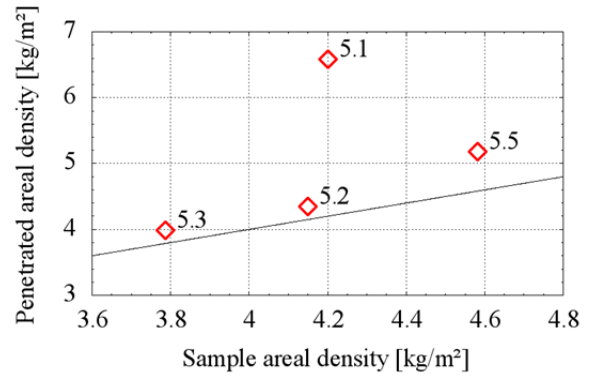


Figure 13. Penetrated areal density plotted vs. sample areal density for the “intermediate layer or reinforced box wall” targets. Solid line is identity.

Major output from the described test campaign is to select the best shielding elements for the next test campaign of the study. However, some very interesting conclusions can be drawn from the described tests:

1. To obtain a good protection, it is advisable to place a certain amount of mass at the outermost location. This can be seen from the experiments of almost all sample types. E.g. heavily reinforced MLI substantially decreases the perforation capability of the resulting fragment cloud.
2. Just adding mass to initial layers may thwart protection, as can be seen by comparing sandwich panel targets 2.1 and 2.2. Here, the heavier sample (2.2) leads to more damage on the witness plates. A more detailed analysis of the two samples showed that due to its stronger inner face sheet, the sandwich panel of Target 2.2 focused the fragment cloud into a narrower angle than the lighter sandwich panel of Target 2.1. The focused fragment cloud subsequently caused more damage to WPI. It should be noted that when impacted by a more damaging particle, 2.2 might perform better.
3. The multi-shock concept as implemented with the internal layer tests in this test campaign is quite powerful. The so-obtained penetrated areal densities are half those of well-performing Al sandwich panels, despite different stand-off distances: For the intermediate layer targets, the distance between bumper plate rear side and witness plate 1 was 100 mm, while for the Al sandwich panel targets the stand-off distance between sandwich panel rear side and witness plate 1 was 250 mm.

6 CONCLUSIONS

In this paper, 20 impact tests of the ReVuS project are described and analyzed. Aim of those tests was to evaluate promising shielding components identified during the study. The components were placed within a set-up that is representative for its occurrence within a spacecraft. The targets were impacted with nominally the same impact conditions above their ballistic limit. The damage potential of the residual fragment cloud was evaluated from damage patterns on witness plates placed behind the targets.

The test results are used to select the most promising targets for the next test campaign, where entire shielding solutions will be tested and compared against each other.

In addition to the selection support, three conclusions can be drawn from the tests that can help future spacecraft designers to optimize their shielding solutions:

1. It is advisable to balance the mass budget available for shielding throughout the shield components. For example, heavily reinforced MLI can lead to significantly less mass required for the module wall to obtain the same level of shielding. Similar results have been found for the sandwich panels.
2. However, additional mass at the wrong spot can thwart the effort for more protection. In the experiments, a sandwich panel with strengthened face sheets caused the exiting fragment to be more focused, leading to more damage to the subsequently impacted witness plate than the impact test of the baseline sandwich panel. This shows that an intelligent shielding approach is required.
3. Finally, the multi-shock concept proved to be very effective. If possible, spacecraft designers should add intermediate layers between the spacecraft outer hull and important components. However, discussions with the ReVuS partners indicate that adding such additional layers may cause significant difficulties for spacecraft integration. Thus, the possibility of using this approach will depend on the considered configuration.

7 ACKNOWLEDGEMENT

The authors thank the European Commission for funding this work under the Seventh Framework Programme (FP7). Funding tag is 262156.

8 REFERENCES

1. Putzar, R., Schäfer, F. & Lambert, M. (2008). Vulnerability of spacecraft harnesses to hypervelocity impacts. *International Journal of Impact Engineering* **35**, 1728-1734.
2. Putzar, R., Schäfer, F., Stokes, H., Chant, R. & Lambert, M. (2006). Vulnerability of spacecraft electronics boxes to hypervelocity impacts. In *Space debris and space traffic management symposium 2005* (Eds. Bendisch, J.), Univelt, San Diego, California, pp307-321. – IAC-05-B6.4.02.
3. Putzar, R., Schäfer, F., Romberg, O. & Lambert, M. (2005). Vulnerability of shielded fuel pipes and heat pipes to hypervelocity impacts. In *Proc. 4th European Conference on Space Debris*, ESA SP-587, ESA Publications Division, Noordwijk, pp459-464.
4. Schäfer, F. K., Putzar, R. & Lambert, M. (2008). Vulnerability of satellite equipment to hypervelocity impacts. In *Proc. 59th International Astronautical Congress*, IAC-08-A6.3.2.
5. Sweeting, M. N., Hashida, Y., Bean, N. P., Hodgart, M. S. & Steyn, H. (2004). CERISE microsatellite recovery from first detected collision in low Earth orbit. *Acta Astronautica* **55**, 139-147.
6. Nasa (2009). Satellite collision leaves significant debris clouds. *Orbital Debris Quarterly News* **13**(2), 1-2.
7. Cougnet, C., David, M., Gergonne, B., Oswald, M., Putzar, R. & Stokes, H. (2012). Solutions to reduce the vulnerability of space systems to impacts of small debris particle. In *Proc. 63rd International Astronautical Congress*, IAC-12.A6.4.4.
8. Christiansen, E. L. (1990). Advanced meteoroid and debris shielding concepts. In *Proc. AIAA/NASA/DOD Orbital Debris Conference*.
9. Christiansen, E. L. (2003). *Meteoroid/Debris Shielding*, NASA Johnson Space Center. – NASA TP-2003-210788.
10. Christiansen, E. L. (1993). Design and performance equations for advanced meteoroid and debris shields. *International Journal of Impact Engineering* **14**, 145-156.